Increased Retinal Expression of the Pro-Angiogenic Receptor GPR91 via BMP6 in a Mouse Model of Juvenile Hemochromatosis

Pachiappan Arjunan,[1,2] Jaya P. Gnanaprakasam,[1] Sudha Ananth,[1] Michelle A. Romej,[1] Veeranan-Karmegam Rajalakshmi,[1] Puttur D. Prasad,[1] Pamela M. Martin,[1] Mariappan Gurusamy,[1] Muthusamy Thangaraju,[1] Yangzom D. Bhutia,[1,3] and Vadivel Ganapathy[1,3]

[1]Department of Biochemistry and Molecular Biology, Georgia Regents University, Augusta, Georgia, United States
[2]Department of Periodontics, Georgia Regents University, Augusta, Georgia, United States
[3]Department of Cell Biology and Biochemistry, Texas Tech University Health Sciences Center, Lubbock, Texas, United States

Correspondence: Vadivel Ganapathy, Department of Cell Biology and Biochemistry, Texas Tech University Health Sciences Center, Lubbock, TX 79430, USA;
vadivel.ganapathy@ttuhsc.edu.

Submitted: June 6, 2015
Accepted: February 13, 2016

Citation: Arjunan P, Gnanaprakasam JP, Ananth S, et al. Increased retinal expression of the pro-angiogenic receptor GPR91 via BMP6 in a mouse model of juvenile hemochromatosis. *Invest Ophthalmol Vis Sci*. 2016;57:1612–1619. DOI:10.1167/iovs.15-17437

Purpose. Hemochromatosis, an iron-overload disease, occurs as adult and juvenile types. Mutations in hemojuvelin (HJV), an iron-regulatory protein and a bone morphogenetic protein (BMP) coreceptor, underlie most of the juvenile type. *Hjv*$^{-/-}$ mice accumulate excess iron in retina and exhibit aberrant vascularization and angiomas. A succinate receptor, GPR91, is pro-angiogenic in retina. We hypothesized that *Hjv*$^{-/-}$ retinas have increased BMP signaling and increased GPR91 expression as the basis of angiomas.

Methods. Expression of GPR91 was examined by qPCR, immunofluorescence, and Western blot in wild-type and *Hjv*$^{-/-}$ mouse retinas and pRPE cells. Influence of excess iron and BMP6 on GPR91 expression was investigated in ARPE-19 cells, and wild-type and *Hjv*$^{-/-}$ pRPE cells. Succinate was used to activate GPR91 and determine the effects of GPR91 signaling on VEGF expression. Signaling of BMP6 was studied by the expression of Smad1/5/8 and pSmad4, and the BMP-target gene Id1. The interaction of pSmad4 with GPR91 promoter was studied by ChIP.

Results. Expression of GPR91 was higher in *Hjv*$^{-/-}$ retinas and RPE than in wild-type counterparts. Unexpectedly, BMP signaling was increased, not decreased, in *Hjv*$^{-/-}$ retinas and RPE. Bone morphogenetic protein 6 induced GPR91 in RPE, suggesting that increased BMP signaling in *Hjv*$^{-/-}$ retinas was likely responsible for GPR91 upregulation. Exposure of RPE to excess iron and succinate as well as BMP6 and succinate increased VEGF expression. Bone morphogenetic protein 6 promoted the interaction of pSmad4 with GPR91 promoter in RPE.

Conclusions. G-protein-coupled receptor 91 is a BMP6 target and *Hjv* deletion enhances BMP signaling in retina, thus underscoring a role for excess iron and hemochromatosis in abnormal retinal vascularization.

Keywords: juvenile hemochromatosis, succinate receptor-GPR91, BMP6 signaling, retinal pigment epithelium, age-related macular degeneration

Hemochromatosis is an autosomal recessive genetic disorder of iron overload caused by mutations in iron-regulatory proteins, namely HLA-like protein involved in iron (FE) homeostasis (HFE), hemojuvelin (HJV), hepcidin (hepatic antimicrobial peptide [Hamp]), ferroportin, and transferrin receptor 2, with a 1 in 300 prevalence of HFE mutations in Caucasians.[1–4] These mutations cause iron accumulation leading to oxidative stress and functional failure in multiple organs. The clinical phenotypes of hemochromatosis include liver cirrhosis, diabetes, cardiomyopathy, and nephropathy. Despite the fact that multiple tissues accumulate iron to detrimental levels, the potential involvement of the retina as a target organ for excessive iron accumulation and functional disruption in this disease has not received much attention. Hemochromatosis occurs in two distinct types: adult and juvenile. Studies from our laboratory using *Hfe*$^{-/-}$ mice (model for adult-type hemochromatosis) have shown that iron accumulates to excessive levels in the retina and that morphological and biochemical alterations do occur in the retina as a consequence of this iron overload.[5–9] In humans, mutations in HFE represent more than 85% of cases of hemochromatosis, and the clinical symptoms occur only in those older than 60 years.

Loss-of-function mutations in *HJV* cause juvenile hemochromatosis. This represents fewer than 5% of cases of hemochromatosis, but it is a rapidly progressive disorder with clinical symptoms arising from excessive iron accumulation in tissues appearing before the age of 30, with the clinical findings including cirrhosis, diabetes, cardiomyopathy, and nephropathy.[10–12] Again, as in the case of HFE mutations, retinal involvement has not been investigated in patients with HJV mutations. We have used *Hjv*$^{-/-}$ mice as a model for juvenile hemochromatosis and demonstrated iron overload and significant morphological alterations in retina in these mice.[13–15] A

Investigative Ophthalmology & Visual Science

distinct difference between *Hfe*$^{-/-}$ and *Hjv*$^{-/-}$ mice is the occurrence of abnormal vascularization in the retina of *Hjv*$^{-/-}$ mice visualized as angiomas.[15] This abnormal phenotype occurs very rarely, if at all, in *Hfe*$^{-/-}$ mice despite excessive iron accumulation. Hemojuvelin is expressed in various retinal cell types, including retinal ganglion cells (RGCs), RPE, Muller cells, and photoreceptor cells.[13] Even though HFE and HJV are both membrane proteins, the former is expressed in the basal membrane and the latter in the apical membrane in RPE.[13,16] However, unlike HFE, which is an integral membrane protein with a transmembrane domain, HJV is anchored to the membrane via glycosylphosphatidylinositol.[17] As such, HJV can be cleaved from the membrane by specific phospholipases and the intact protein can be released in a soluble form. The membrane-anchored HJV is a coreceptor for bone morphogenetic proteins (BMPs) and potentiates BMP signaling.[18] The soluble form of HJV binds BMPs and prevents BMP signaling.[17] This suggests that the relative abundance of the two forms of HJV in a given tissue would determine the final outcome of BMP signaling. Hemojuvelin facilitates the expression of the iron-regulatory hormone hepcidin via BMP signaling.[18] Although BMP2, BMP4, and BMP6 all induce hepcidin expression in vitro in an HJV-dependent manner,[18] BMP6 seems to be solely responsible in vivo.[19] However, HJV does not mediate BMP signaling on its own but requires BMP receptors. Bone morphogenetic protein signaling involves phosphorylation of Smad protein complex resulting in its nuclear translocation to induce the target genes.

G-protein-coupled receptor 91 (GPR91) is pro-angiogenic in retina and serves as a cell-surface receptor for succinate.[20] It is expressed in RGCs and RPE.[6,21,22] Succinate is an intermediate in the Krebs cycle that occurs in mitochondria, and its levels rise during hypoxia and oxidative stress. G-protein-coupled receptor 91 responds to increased succinate levels and triggers vascular proliferation via increased expression of VEGF.[21,22] Abnormal expression of GPR91 in retina is likely to have significant consequences in terms of angiogenesis. Previous studies have shown that GPR91 expression is increased in the *Hfe*$^{-/-}$ mouse retina.[6] As abnormal retinal vascularization and angiogenesis are seen in *Hjv*$^{-/-}$ mice more frequently and more markedly than in *Hfe*$^{-/-}$ mice, we thought it was important to interrogate GPR91 expression in this mouse model of juvenile hemochromatosis.

Materials and Methods

Materials

The human RPE cell line ARPE-19 was obtained from the American Type Culture Collection (Manassas, VA, USA). TRIzol reagent and Dulbecco's modified Eagle's medium (DMEM)/F12 culture medium were purchased from Life Technologies (Grand Island, NY, USA); iScript cDNA synthesis kit from Bio-Rad Laboratories (Hercules, CA, USA); DreamTaq Green PCR Master Mix from Thermo Scientific (Pittsburgh, PA, USA); fetal bovine serum, penicillin, and streptomycin from Life Technologies (Grand Island, NY, USA); rabbit polyclonal anti-GPR91 antibody from Alpha Diagnostic International (San Antonio, TX, USA); antibodies against Smad1/5 and phospho-Smad1/5/8 from Cell Signaling Technology, Inc., (Danvers, MA, USA); antibody against phospho-Smad4 from Abgent, Inc., (San Diego, CA, USA); and secondary antibodies (goat anti-rabbit IgG conjugated with Alexa Fluor 568 and goat anti-rabbit IgG coupled to Alexa Fluor 488) from Molecular Probes (Carlsbad, CA, USA).

Animals

Breeding pairs of HJV knockout (*Hjv*$^{-/-}$) mice were originally obtained from Nancy Andrews, MD, Duke University. These mice are on SvJ/129 genetic background; therefore, wild-type SvJ/129 mice were used as corresponding controls. Age-matched wild-type and knockout mice were used. The mice were maintained on standard laboratory chow and water ad libitum. All procedures involving mice were approved by the Institutional Animal Care and Use Committee of the Georgia Regents University and were in accordance with the ARVO statement for the use of animals in ophthalmic and vision research.

Culture and Treatment of Cells

Wild-type and knockout mouse pups (age: postnatal day 18) were used to establish primary cultures of RPE cells (pRPE) as described in our previous publications.[5–7,14] The cells were kept in culture only for three to four passages, and the experiments were performed with cells in the second or third passage. Mouse pRPE cells and ARPE-19 cells were seeded in 10-cm^2 culture dishes at a density of approximately 1×10^6 cells per dish in DMEM/F12K medium supplemented with 10% fetal bovine serum, 100 units/mL penicillin, and 100 μg/mL streptomycin and cultured for 24 hours. The cells were grown to 70% confluence in serum-starved media for 8 hours. Fresh culture medium was then added to cells with and without ferric ammonium citrate (FAC; 100 μg/mL), and the cells were cultured for 72 hours. During the final 16 hours of this treatment, culture medium was replaced with fresh corresponding medium (i.e., with or without FAC) containing 2 mM succinate. The concentration of FAC and the treatment time were selected based on our previously published reports to cause iron overload in cells.[6,9] Treatment of cells with BMP6 was carried out following the 8-hour treatment of the cells in the serum-starved medium. The cells were exposed to fresh medium containing 2 mM succinate with and without recombinant human BMP6 (2 μg/mL) for 24 hours. RNA was prepared from control and treated cells and used for RT-PCR, quantitative PCR (qPCR), and immunofluorescence.

Reverse-Transcriptase PCR and Real-Time PCR

To prepare RNA from posterior segments of the eye, cornea and lens were removed, and the posterior cup with retina was collected. In some experiments, the neural retina was peeled off from the eyecup, leaving behind the RPE/eyecup. RNA was extracted from the whole retina, neural retina, RPE/eyecup, wild-type and *Hjv*$^{-/-}$ mouse pRPE cells, and ARPE-19 cells using TRIzol reagent. Complementary DNA was synthesized using the iScript cDNA synthesis kit. Reverse-transcriptase PCR was carried out under optimal conditions specific for PCR primer pairs. The following primers were used: mouse GPR91 forward 5′-TGTGAGAATTGGTTGGCAACAG-3′ and reverse 5′-TCGGTCCATGCTAATGACAGTG-3′; human GPR91 forward 5′-GCAACCGATATGTGCTTCATGCCA-3′ and reverse 5′-TGCAGAAGGTGTTCTCGGAAAGGA-3′; mouse Hjv forward 5′-GGCTGAGGTGGACAATCTTC-3′ and reverse 5′-GAACAAAGAGGGCCGAAAG-3′; mouse hepcidin forward 5′-GCACCACCTATCTCCATCAACAGA-3′ and reverse 5′-GGTCAGGATGTGGCTCTAGGCTAT-3′; mouse Id1 forward 5′-CGACTACATCAGGGACCTGCA-3′ and reverse 5′-GAACACATGCCGCCTCGG-3′; mouse VEGF forward 5′-GTCCGATTGAGACCCTGGTG-3′ and reverse 5′-ATCCGCATGATCTGCATGGT-3′; human VEGF forward 5′-CTACCTCCACCATGCCAAGT-3′ and reverse 5′-GCAGTAGCTGCGCTGATAGA-3′; human HPRT1 forward 5′-GCGTCGTGATTAGCGATGATGAAC-3′ and reverse 5′-CCTCCCATCTCCTTCATGACATCT-3′; 18S-rRNA forward 5′-CCCGTTGAACCCCATTCGT-3′ and reverse 5′-GCCTCACTAAACCATCCAATCGGTA-3′. Real-time amplifications were run in triplicate on 96-well plates. Genes in each sample were normalized to that of either HPRT1 or 18S-rRNA, and the data

were analyzed for relative expression of a given target gene in treated cells compared with control cells or in *Hjv*-null mouse retinal tissues compared with wild-type mouse retinal tissues by $2^{-\Delta\Delta Ct}$ method.

Immunofluorescence Analysis

The eyes were embedded in Optimal Cutting Temperature compound (Crystalgen, Inc., Commack, NY, USA). Tissues were cut into 10-µm frozen sections and fixed in 4% paraformaldehyde. Retinal sections were blocked with 1x Power Block and incubated overnight at 4°C with a polyclonal anti-GPR91 antibody (1:100). Negative controls involved omission of the primary antibody. Sections were rinsed and incubated for 1 hour with a secondary antibody (goat anti-rabbit IgG) conjugated with Alexa Fluor 568. Coverslips were mounted after staining with 4′,6-diamidino-2-phenylindole (Sigma-Aldrich Corp., St. Louis, MO, USA) nuclear stain and sections were examined with a laser-scanning confocal microscope (Carl Zeiss, Oberkochen, Germany). Cultured cells were processed on coverslips, fixed in methanol, and used for immunofluorescence analysis of Hjv, GPR91, or phospho-Smad4 in a similar manner.

Western Blot

Protein lysates were prepared from wild-type and *Hjv*$^{-/-}$ mouse pRPE cells using RIPA buffer (Sigma-Aldrich Corp.). The same was done with neural retina or RPE/eyecup from wild-type and *Hjv*$^{-/-}$ mice. The protein extracts (20 µg) were subjected to electrophoresis on 10% polyacrylamide gel and then transferred onto a nitrocellulose membrane, probed with specific polyclonal antibodies against GPR91, phospho-Smad1/5/8, or total Smad1/5. Positive bands were detected with appropriate secondary antibodies coupled to horseradish peroxidase. Signals were developed with an enhanced Chemiluminescence detection kit (Thermo Fisher Scientific, Inc., Waltham, MA, USA). Beta-actin was used as an internal control for protein loading. The levels of target protein were quantified by densitometry and normalized with the corresponding internal control.

Chromatin Immunoprecipitation (ChIP)

Chromatin immunoprecipitation was performed using a commercial kit (Millipore, Billerica, MA, USA). Cultured ARPE-19 cells were treated with and without BMP6 for 24 hours as described above and then fixed in 1% formaldehyde for 20 minutes. Formaldehyde crosslinks DNA to proteins bound to specific DNA fragments. The cells were lysed and sonicated to produce 200- to 500-bp chromosomal DNA fragments. After preclearance with salmon sperm DNA, BSA, and protein A-agarose slurry, the supernatants were incubated overnight with the antibody against p-Smad4. The antibody was omitted in the negative control. Protein A-agarose beads were used to precipitate the antibody-pSmad4-DNA complexes. The precipitates were washed and DNA was eluted. The DNA-protein crosslinks were reversed at 65°C and the DNA purified. The amount of GPR91-promoter DNA in the p-Smad4-immunoprecipitates was analyzed by RT-PCR and quantified by real-time PCR using site-specific primer sets (forward 5′-TTTGGAGCACAAGGTGACTT-3′ and reverse 5′-TGCCAAAGAATTCTGCTTATTGT-3′). The primers were selected for the target site in the GPR91 promoter containing hexameric CAGACA sequence specific for the Smad-binding element (SBE).[23]

Statistical Analysis

Experiments were repeated at least thrice. Data are represented as means ± SE. Statistical analysis was done using Student's *t*-test. A P value < 0.05 was considered statistically significant.

Results

Expression of GPR91 in *Hjv*$^{-/-}$ Mouse Retina

We performed RT-PCR for GPR91 using RNA from neural retina, RPE/eyecup, and pRPE of wild-type and *Hjv*$^{-/-}$ mice. G-protein-coupled receptor 91 mRNA levels were higher in neural retina, RPE/eyecup, and pRPE cells from *Hjv*$^{-/-}$ mice than from wild-type mice (Fig. 1A). Next we quantified GPR91 mRNA levels by qPCR and confirmed the upregulation of the receptor mRNA in *Hjv*$^{-/-}$ mouse retina and pRPE (Fig. 1B). The increase in the steady-state levels of GPR91 mRNA in *Hjv*$^{-/-}$ mouse retina and pRPE was approximately 2-fold compared with wild-type mouse retina and pRPE. We then performed Western blot using the protein lysates from neural retina, RPE/eyecup, and pRPE cells obtained from wild-type and *Hjv*$^{-/-}$ mice. G-protein-coupled receptor 91 protein levels were increased in *Hjv*$^{-/-}$ mouse retina and RPE than in corresponding tissues from wild-type mice (Fig. 1C). These results were corroborated by immunofluorescence analysis of GPR91 protein with pRPE cells (Fig. 1D). These data demonstrate clearly that deletion of *Hjv* in mice results in upregulation of GPR91 in the retina and RPE.

GPR91 is Upregulated by BMP6 in Cultured RPE Cells

Very little is known on the factors that regulate the expression of GPR91. We have shown previously that GPR91 expression is increased in the retina and RPE of *Hfe*$^{-/-}$ mice.[6] We find a similar phenomenon in the present study in *Hjv*$^{-/-}$ mice. Excessive iron accumulation in retina is a common phenotype in these two mouse models.[8] Both Hfe and Hjv target the gene coding for the iron-regulatory hormone hepcidin in liver via BMP6 signaling[8,15] and that deletion of either Hfe or Hjv in mice interferes with BMP6 signaling with resultant decrease in hepcidin expression in the liver.[17–19] Based on these findings, we thought that the disrupted BMP6 signaling in *Hjv*$^{-/-}$ mice might be responsible for the upregulation of GPR91 in retina. Our hypothesis was that BMP6 was a negative regulator of GPR91 expression and that the observed upregulation of GPR91 in *Hjv*$^{-/-}$ mouse retina and RPE was due to decreased BMP6 signaling that has been reported in *Hjv*$^{-/-}$ mouse liver. To test this, we examined the effect of BMP6 on GPR91 expression in mouse pRPE cells (wild-type) and in ARPE-19 cells (Fig. 2). Contrary to our prediction, exposure of RPE cells to BMP6 did not decrease, but instead increased, the expression of the receptor. This phenomenon was seen at both mRNA (Figs. 2A, 2B) and protein levels (Fig. 2C). These findings were surprising and unexpected; these data suggested that deletion of *Hjv* in mice might actually lead to an increase in BMP6 signaling in retina contrary to what has been reported in liver.

Evidence of Increased BMP-Smad 1/5/8 Signaling in *Hjv*$^{-/-}$ Retina

To examine if deletion of *Hjv* has opposite effects on BMP6 signaling in retina versus liver, we monitored the expression of a well-known target gene for BMP6, namely *Id1*, in wild-type and *Hjv*$^{-/-}$ mouse retina and liver. We found the expression of Id1 to be upregulated in *Hjv*$^{-/-}$ mouse retina compared with wild-type retina (Fig. 3A); in contrast, the expression of Id1 was reduced in *Hjv*$^{-/-}$ mouse liver compared with wild-type mouse liver (Fig. 3A), confirming the findings in the literature. Our data showed that the impact of *Hjv* deletion on BMP6 signaling is not the same in retina and liver. Bone morphogenetic protein 6 signaling is actually increased in *Hjv*$^{-/-}$ mouse retina compared with wild-type mouse retina. We confirmed

Investigative Ophthalmology & Visual Science

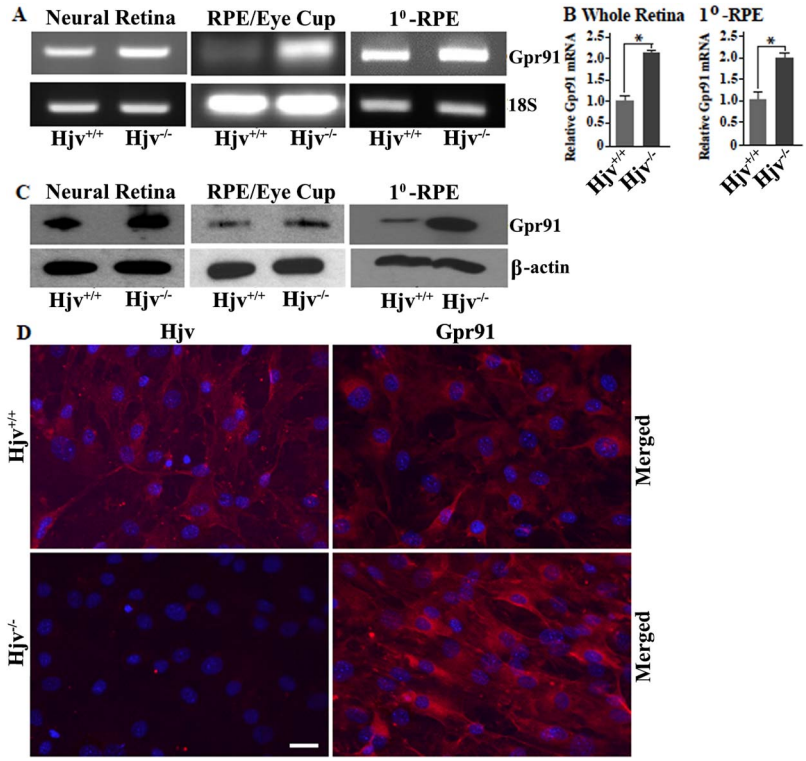

Figure 1. Increased expression of GPR91 in *Hjv*$^{-/-}$ mouse retina compared with wild-type mouse retina. (**A**) Reverse-transcriptase PCR analysis of GPR91 mRNA expression in neural retina, RPE/eyecup, and 1°RPE cells from wild-type (*Hjv*$^{+/+}$) and *Hjv*$^{-/-}$ mice. The experiment was repeated three times with similar results. (**B**) G-protein-coupled receptor 91 mRNA levels in whole retina and 1°RPE cells from *Hjv*$^{+/+}$ and *Hjv*$^{-/-}$ mice were determined by real-time PCR; 18S rRNA was used as an internal control. The experiment was repeated three times with independent RNA samples and data are presented as means ± SE. $^{*}P < 0.05$. (**C**) Western blot analysis of GPR91 using protein lysates from *Hjv*$^{+/+}$ and *Hjv*$^{-/-}$ mouse neural retina, RPE/eyecup, and 1°RPE cells. The blot was developed using a primary antibody specific to GPR91. Beta-actin was used as an internal control. The experiment was repeated three times with similar results. 1°-RPE, primary RPE. (**D**) Immunofluorescence analysis of GPR91 protein expression in 1°RPE cells from *Hjv*$^{+/+}$ and *Hjv*$^{-/-}$ mice. Immunofluorescence analysis of Hjv protein is also shown. *Scale bar*: 50 μm. Images are representative of three independent experiments.

this conclusion by examining the phosphorylation status of Smad1/5/8, the downstream component in BMP6 signaling pathway, by Western blot in wild-type and *Hjv*$^{-/-}$ mouse retinas. The level of phospho-Smad1/5/8 was significantly increased in *Hjv*$^{-/-}$ mouse retina compared with wild-type mouse retina with no noticeable change in the level of total Smad1/5/8 (Fig. 3B).

Upregulation of GPR91 by BMP6 in RPE Cells Independent of Hjv

Although the biological functions of BMP6 are differentially modulated by soluble and membrane-bound HJV, these functions are not obligatorily dependent on HJV. We assessed the influence of BMP6 on the expression of GPR91 and hepcidin in pRPE cells from wild-type mice and *Hjv*$^{-/-}$ mice. Treatment of the cells with BMP6 increased the expression of genes in both wild-type as well as *Hjv*$^{-/-}$ RPE cells (data not shown), indicating that the ability of BMP6 to induce GPR91 in RPE cells is not obligatorily dependent on the presence of Hjv. The same is true with regard to BMP6-induced upregulation of hepcidin.

Evidence of GPR91 as a Direct Target Gene for BMP6 Signaling in RPE Cells

To further corroborate our conclusion that GPR91 is a direct target for BMP6 in RPE, we examined the influence of BMP6 on the phosphorylation status of Smad4 and its nuclear localization. Bone morphogenetic protein 6 signaling involves the following: engagement of BMP receptor with its ligand → phosphorylation of Smad1/5/8 → phosphorylation of Smad4 → translocation of the pSmad4/pSmad1/5/8 complex into the nucleus → binding of the complex to the SBE in the target gene → induction of transcription of the target gene. To determine if this signaling pathway is responsible for the induction of GPR91 by BMP6, we first monitored the status and location of phospho-Smad4 in ARPE-19 cells in response to BMP6 treatment (Fig. 4A). We found that exposure of the cells to BMP6 increased the cellular levels of pSmad4, which is almost completely localized to the nucleus. We then performed ChIP assay to determine if pSmad4 associated with GPR91 promoter (Figs. 4B, 4C). Immunoprecipitation of nuclear extracts with antibody specific for phospho-Smad4 did bring down GPR91 promoter fragment containing the SBE element. The association of pSmad4 with the promoter was significantly greater in BMP6-treated cells than in untreated cells.

Relevance of GPR91 Signaling to VEGF Expression in Response to Iron Overload and BMP6

G-protein-coupled receptor 91–succinate signaling is pro-angiogenic in retina and is associated with increased expression of VEGF, the principal mediator of retinal vessel growth.[17] Therefore, subsequent to our observations that *Hjv*$^{-/-}$ RPE cells upregulate GPR91 via BMP6, we asked whether these processes lead to increased VEGF expression. For this, we used wild-type mouse pRPE cells and the human ARPE-19 cell line.

Investigative Ophthalmology & Visual Science

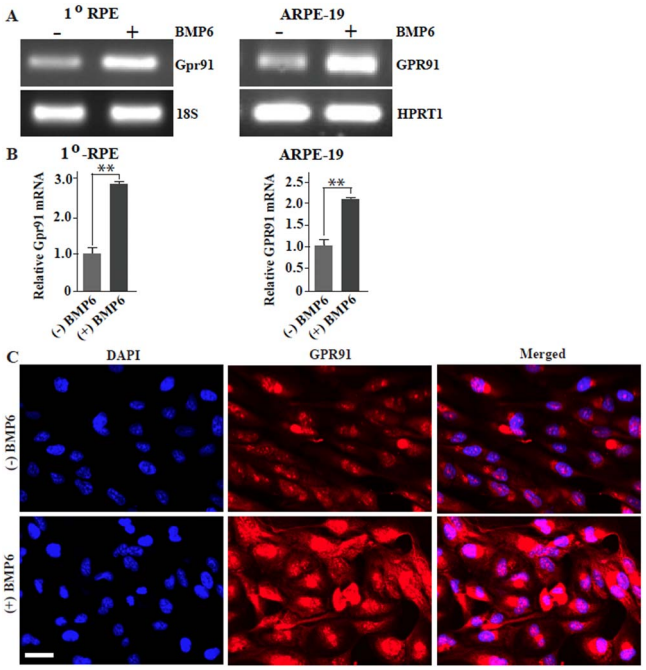

Figure 2. Upregulation of GPR91 expression in mouse and human RPE (ARPE-19 cell line) cells by treatment with BMP6. (**A**, **B**) Mouse (wild-type) 1°RPE cells and ARPE-19 cells were treated without (–) or with (+) BMP6 (2 μg/mL) in the regular culture medium for 24 hours. RNA was isolated from control and treated cells and used for RT-PCR (**A**) and real-time PCR (**B**); 18S or HPRT1 was used as internal control. Data for real-time PCR are presented as means ± SE from three independent experiments. $^{**}P < 0.01$. (**C**) Immunofluorescence analysis of GPR91 protein in control and BMP6-treated ARPE-19 cells. The experiment was repeated twice with similar results. *Scale bar*: 50 μm.

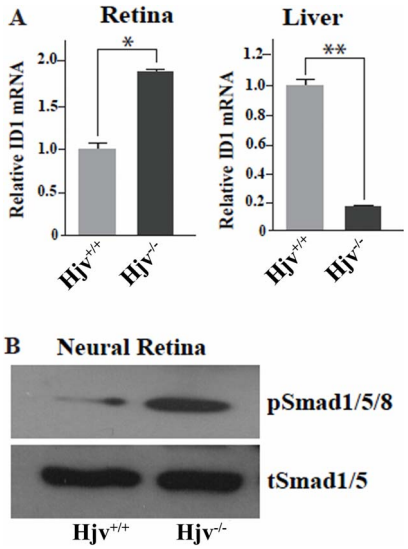

Figure 3. Differential impact of *Hjv* deletion in mice on Smad signaling in retina versus liver. (**A**) RNA was isolated from retina and liver collected from wild-type ($Hjv^{+/+}$) and knockout ($Hjv^{-/-}$) mice and used for real-time PCR to monitor mRNA levels for ID1, a target for Smad signaling. The experiment was repeated with three biologically independent RNA samples. $^{*}P < 0.05$; $^{**}P < 0.01$. (**B**) Western blot analysis of phospho-Smad1/5/8 and total Smad1/5 in protein lysates prepared from $Hjv^{+/+}$ and $Hjv^{-/-}$ mouse retinal tissues. The experiment was repeated twice with similar results.

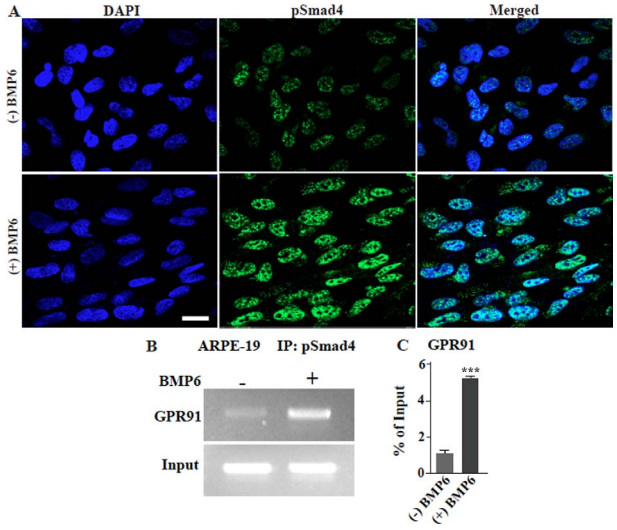

Figure 4. G-protein-coupled receptor 91 is a target for BMP6 signaling. (**A**) ARPE-19 cells were treated with or without BMP6 (2 μg/mL) for 24 hours and then used for analysis of phospho-Smad4 protein using a laser-scanning confocal microscope. The image shown is representative of four different experiments. *Scale bar*: 50 μm. (**B**) Binding of phospho-Smad4 to GPR91 promoter as demonstrated by ChIP. ARPE-19 cells were treated with or without BMP6 (2 μg/mL) for 24 hours and then nuclear preparations were made from control and treated cells for use in ChIP assay. (**C**) Quantification of phospho-Smad4 occupancy on *GPR91* promoter in control and BMP6-treated ARPE-19 cells. Data are presented as means ± SE for three independent ChIP experiments. $^{***}P < 0.001$.

First, we examined the role of iron overload in the GPR91-VEGF axis (Figs. 5A–D). Loading the cells with excess iron via exposure to FAC induced VEGF expression in the presence of succinate in mouse and human RPE cells. As excess iron is known to induce GPR91 expression, we conclude that excess iron induces VEGF expression via GPR91-succinate signaling. Similarly, we examined the role of BMP6 in the GPR91-VEGF axis (Figs. 5E–H). Exposure of the cells to BMP6 induced VEGF expression in the presence of succinate in mouse and human RPE cells. Because we have already established that BMP6 induces GPR91, we conclude that BMP6 induces VEGF expression in RPE cells via GPR91-succinate signaling.

We performed similar experiments with primary RPE cells from wild-type and $Hfe^{-/-}$ mice (Fig. 6A). Exposure to excess iron in the form of FAC increased VEGF-A mRNA in wild-type primary RPE cells. As deletion of Hfe leads to increased accumulation of iron, VEGF-A mRNA levels were higher in $Hfe^{-/-}$ RPE cells than in wild-type RPE cells irrespective of whether or not the knockout cells were exposed to FAC (Fig. 6A). We then examined the involvement of GPR91 in VEGF expression induced by the combination of FAC and BMP6. For this, we used ARPE-19 cells and monitored the expression of VEGF by Western blot (Fig. 6B). In control ARPE-19 cells, succinate significantly increased the expression of VEGF-A, but this effect was markedly higher in cells that had been exposed to FAC and BMP6. These data demonstrate that exposure of RPE cells to excess iron and BMP6 increase the expression of GPR91 and that subsequent treatment with succinate, the GPR91 agonist, enhances VEGF expression.

Discussion

In recent years, three novel receptors have been identified that are activated by specific intermediates found in critical

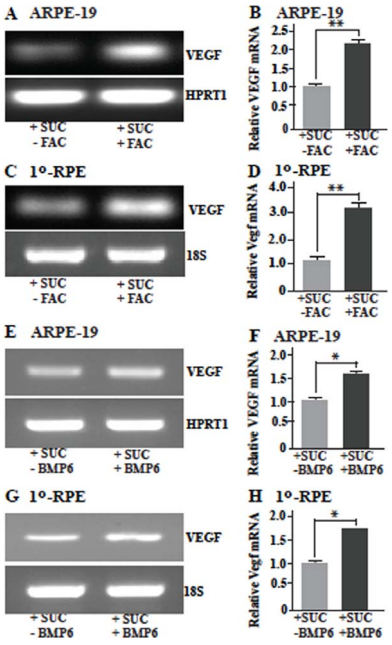

Figure 5. Promotion of VEGF expression in ARPE-19 cells and wild-type mouse 1°RPE cells by iron- and BMP6-induced GPR91. (**A–D**) ARPE-19 cells and wild-type mouse 1°RPE cells were cultured for 72 hours in the presence of FAC (100 μg/mL) to load the cells with excess iron. During the final 16 hours of this treatment, the medium was replaced with respective medium (i.e., with or without FAC) containing succinate (2 mM). RNA was isolated from the cells at the end of this treatment and used for RT-PCR (**A**, **C**) and real-time PCR (**B**, **D**) to monitor the levels of VEGF mRNA. Reverse-transcriptase PCR was repeated three times with comparable results. Real-time PCR was done with three independent RNA preparations and data are presented as means ± SE. $^{**}P < 0.01$. (**E–H**) ARPE-19 cells and wild-type mouse 1°RPE cells were cultured for 24 hours in the presence of succinate (2 mM) with and without BMP6 (2 μg/mL). RNA was isolated from the cells at the end of this treatment and used for RT-PCR (**E**, **G**) and real-time PCR (**F**, **H**) to monitor the levels of VEGF mRNA. Reverse-transcriptase PCR was repeated three times with comparable results. Real-time PCR was done with three independent RNA preparations and data are presented as means ± SE. $^{*}P < 0.05$; 18S RNA or HPRT1 RNA was used as the internal control.

metabolic pathways: GPR91 activated by the citric acid cycle intermediate succinate,[20] GPR81 activated by the ubiquitous metabolite lactate,[24] and GPR109A activated by the ketone body β-hydroxybutyrate.[25] These receptors are collectively called metabolite receptors, which play significant roles in a variety of critical biological functions; these receptors affect intracellular signaling pathways in response to changes in the levels of their metabolite agonists in the extracellular fluid. Because the changes in circulating levels of these metabolites indicate alterations in the rates of important metabolic pathways in the organism as a whole, these receptors provide an important link to cellular metabolism in an autocrine and/or paracrine manner. They are also indicators of cellular energy status and oxygen availability. Hypoxia and disruptions in mitochondrial function are expected to increase the circulating levels of succinate and lactate; similarly, inability of the organism to use glucose as the energy source is expected to increase fatty acid oxidation as an alternative energy source and hence enhance the production of β-hydroxybutyrate in ketogenic organs such as liver.

Retina expresses all three metabolite receptors (Pachiappan A, et al. *IOVS* 2014;55:ARVO E-Abstract 6337; Ganapathy V, et al. *IOVS* 2014;55:ARVO E-Abstract 2954).[6,21,26] The present study focuses on GPR91 expression in response to excessive iron accumulation in retina. The connection between GPR91 and iron is important for several reasons. Cellular iron levels and hypoxia are tightly linked through the oxygen-carrying molecule hemoglobin. Iron is also related to mitochondrial function, not only in metabolic pathways, such as the citric acid cycle and electron transport chain, but also in heme biosynthesis. Therefore, alterations in cellular iron status are expected to affect the cellular levels of succinate, the agonist for GPR91. Several studies have shown that GPR91 is pro-angiogenic in retina with ability to induce VEGF synthesis and secretion[6,21]; this makes sense considering the central role of iron and oxygen status in the process and the iron-dependent induction of the receptor. Congruent with this link among GPR91, iron, hypoxia, and mitochondrial function, deletion of *GPR91* in mice leads to defective retinal angiogenesis,[22] confirming its pro-angiogenic role. Similarly, GPR91 signaling is increased in retina in diseases associated with abnormal retinal neovascularization (diabetes and retinopathy of prematurity).[27]

The present study demonstrates a link between the iron-overload disease hemochromatosis and GPR91 in retina. We have already shown that the retinal expression of this receptor is upregulated in *Hfe*$^{-/-}$ mice (adult-type model).[6] Here, we demonstrate a similar phenomenon in *Hjv*$^{-/-}$ mice, a model for the juvenile type. This finding in itself is not surprising because excessive iron accumulation in the retina is a hallmark of both mouse models.[14,25] The importance of the present study lies in the discovery that BMP signaling is involved in the process. This is the first report describing the regulation of GPR91 by BMP6 and its connection to hemochromatosis. The significance of these findings is 2-fold: first, we demonstrate that GPR91 is a direct target for BMP6 signaling, and second, BMP signaling is increased in *Hjv*$^{-/-}$ mouse retina. The former finding represents a hitherto unknown regulatory control of GPR91 expression and the latter finding represents a surprising phenomenon that is in contrast to the status of BMP signaling in liver in this mouse model. The decrease in BMP signaling in liver and the increased BMP signaling in retina in the same *Hjv*$^{-/-}$ mouse model underscores the complex processes involved in the regulation of BMP signaling by HJV. Because the membrane-bound and the soluble forms of HJV have opposite effects on BMP signaling, the relative levels of these two forms would be a determinant of net BMP signaling in a given tissue. Apparently, these relative levels differ in liver versus retina. A serine protease (matriptase2 or TMPRSS6) expressed robustly in the retina[28] is responsible for generating the soluble form of HJV. It is possible that levels of this enzyme vary markedly between liver and retina. Irrespective of the exact mechanism, it is reasonable to conclude that the relative levels of membrane-bound and soluble forms of HJV in liver and retina are such that in wild-type mice, Hjv promotes net BMP signaling in the former tissue but suppresses it in the latter. When *Hjv* is deleted, BMP signaling is suppressed in liver, whereas it is increased in retina.

Bone morphogenetic proteins belong to the TGF-β superfamily of ligands.[29,30] Bone morphogenetic protein 6 binds to type I (BMPRI) and II (BMPRII) cell-surface receptors and to the coreceptor HJV. The engagement of the receptor complex with BMP6 increases the kinase activity of the type II receptor, resulting in the phosphorylation of the type I receptor, which in turn activates the Smad signaling cascade through phosphorylation of Smad1/5/8. The phosphorylated Smad1/5/8 then associates with Smad4 to form a heteromeric complex that translocates to the nucleus and promotes transcription of target genes (ID1 and hepcidin).[29,30] Smad4 exists either in a constitutively phosphorylated form or is phosphorylated in response to BMPR activation. The present study provides

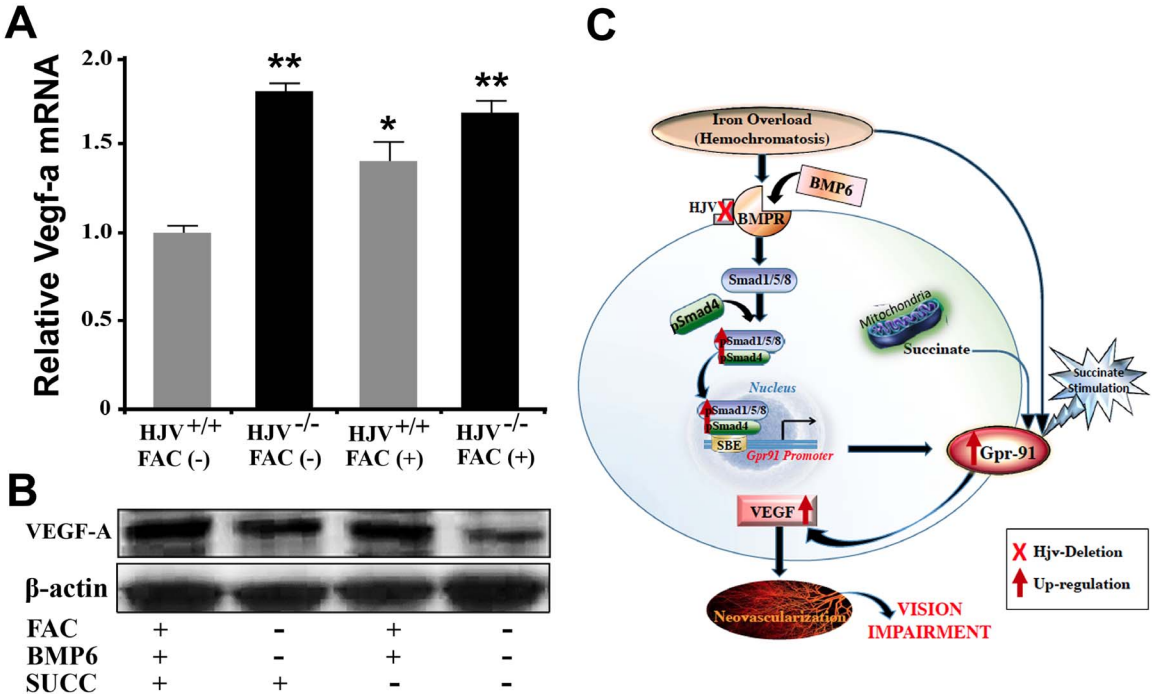

Figure 6. Role of excess iron in the induction of VEGF in *Hfe*$^{-/-}$ RPE cells and the involvement of the succinate receptor GPR91 in the process. (**A**) 1°RPE cells from wild-type and *Hfe*$^{-/-}$ mice were treated with or without FAC (100 μg/mL) for 24 hours. RNA from the cells was then used for real-time PCR to monitor the levels of VEGF-A mRNA (three biological replicates). Data are given as means ± SE. $^{*}P < 0.05$ compared with wild-type cells in the absence of FAC; $^{**}P < 0.01$ compared with wild-type cells in the absence of FAC. (**B**) ARPE-19 cells were cultured for 72 hours in the presence or absence of FAC (100 μg/mL) with or without succinate (2 mM) for 24 hours. During the final 16 hours of this treatment, the cells were exposed to respective fresh medium with or without BMP6 (2 μg/mL). Protein lysates from the cells were then used for Western blot to monitor the levels of VEGF-A protein. Data are from a representative experiment; the experiment was repeated four times with similar results. (**C**) A schematic of the signaling pathways involved in the induction of GPR91 in hemochromatosis RPE and the consequences of the induction in terms of VEGF expression and vascularization.

evidence for most of these steps in the BMP6 signaling cascade for the induction of GPR91, which includes increase in the cellular levels of phospho-Smad1/5/8, nuclear levels of phospho-Smad4, and binding of phospho-Smad4 to *GPR91* promoter. This pathway is activated in retina when the iron-regulatory protein HJV is not functional as occurs in the genetic iron-overload disease hemochromatosis. The increased density of GPR91 on the cell surface in iron-overloaded RPE cells in *Hfe*$^{-/-}$ mice leads to increased expression of VEGF in response to the agonist succinate, which then results in neovascularization and consequent retinal dysfunction. These pathways are described schematically in Figure 6C.

Our findings that excessive iron accumulation in retina in hemochromatosis induces GPR91 expression have clinical significance to diseases such as diabetes and AMD that show abnormal proliferation of blood vessels in retina. Patients with these diseases have more iron in their retinas than control subjects,[31–33] suggesting that iron-induced upregulation of GPR91 might contribute to the blood vessel pathology. There are no data in the literature on whether patients with hemochromatosis have abnormal blood vessel proliferation in the retina, but we strongly believe that it might be the case. The mouse models of hemochromatosis (*Hfe*$^{-/-}$ and *Hjv*$^{-/-}$) have evidence of abnormal neovascularization in the retina, the magnitude of this pathology being much greater in *Hjv*$^{-/-}$ than in *Hfe*$^{-/-}$ mice.[15] Based on these observations, we hypothesize that hemochromatosis might be an important modifier of disease progression in patients with AMD.

The data showing that GPR91 expression in retina is regulated by BMP signaling is also important to retinal pathology associated with diabetes, AMD, and hemochromatosis, excessive iron in this tissue being a common factor in all three diseases. Bone morphogenetic protein 6 signaling plays a critical role in iron homeostasis[34] and *BMP6*-null mice show evidence of abnormal iron accumulation in retina.[35] Bone morphogenetic protein 6 is expressed in RPE, a major site of pathology in AMD, in response to iron.[35] Therefore, the discovery that GPR91 is a target for BMP6 signaling in retina has clinical and therapeutic significance. Pharmacological blockade of the BMP6-GPR91 signaling pathway might have potential in the treatment of array of diseases exhibiting abnormal blood vessel proliferation in the retina.

Acknowledgments

Supported by grant from the National Eye Institute (EY019672).

Disclosure: **P. Arjunan**, None; **J.P. Gnanaprakasam**, None; **S. Ananth**, None; **M.A. Romej**, None; **V.-K. Rajalakshmi**, None; **P.D. Prasad**, None; **P.M. Martin**, None; **M. Gurusamy**, None; **M. Thangaraju**, None; **Y.D. Bhutia**, None; **V. Ganapathy**, None

References

1. Andrews NC, Levy JE. Iron is hot: an update on the pathophysiology of hemochromatosis. *Blood*. 1998;92:1845–1851.
2. Babitt JL, Lin HY. The molecular pathogenesis of hereditary hemochromatosis. *Semin Liver Dis*. 2011;31:280–292.
3. Santos PC, Krieger JE, Pereira AC. Molecular diagnostic and pathogenesis of hereditary hemochromatosis. *Int J Mol Sci*. 2012;13:1497–1511.

4. Barton JC. Hemochromatosis and iron overload: from bench to clinic. *Am J Med Sci*. 2013;346:403–412.
5. Gnanaprakasam JP, Thangaraju M, Liu K, et al. Absence of iron-regulatory protein Hfe results in hyperproliferation of retinal pigment epithelium: role of cysteine/glutamate exchanger. *Biochem J*. 2009;424:243–252.
6. Gnanaprakasam JP, Ananth S, Prasad PD, et al. Expression and iron-dependent regulation of succinate receptor GPR91 in retinal pigment epithelium. *Invest Ophthalmol Vis Sci*. 2011; 52:3751–3758.
7. Gnanaprakasam JP, Reddy SK, Veeranan-Karmegam R, Smith SB, Martin PM, Ganapathy V. Polarized distribution of heme transporters in retinal pigment epithelium and their regulation in the iron-overload disease hemochromatosis. *Invest Ophthalmol Vis Sci*. 2011;52:9279–9286.
8. Gnanaprakasam JP, Veeranan-Karmegam R, Coothankandaswamy V, et al. Loss of Hfe leads to progression of tumor phenotype in primary retinal pigment epithelial cells. *Invest Ophthalmol Vis Sci*. 2013;54:63–71.
9. Ananth S, Gnanaprakasam JP, Bhutia YD, et al. Regulation of the cholesterol efflux transporters ABCA1 and ABCG1 in retina in hemochromatosis and by the endogenous siderophore 2,5-dihydroxybenzoic acid. *Biochim Biophys Acta*. 2014;1842:603–612.
10. Roetto A, Camaschella C. New insights into iron homeostasis through the study of non-HFE hereditary haemochromatosis. *Best Pract Res Clin Haematol*. 2005;18:235–250.
11. Pietrangelo A. Non-HFE hemochromatosis. *Semin Liver Dis*. 2005;25:450–460.
12. Wallace DF, Subramaniam VN. Non-HFE haemochromatosis. *World J Gastroenterol*. 2007;13:4690–4698.
13. Gnanaprakasam JP, Zhang M, Martin PM, Atherton SS, Smith SB, Ganapathy V. Expression of the iron-regulatory protein haemojuvelin in retina and its regulation during cytomegalovirus infection. *Biochem J*. 2009;419:533–543.
14. Gnanaprakasam JP, Tawfik A, Romej M, et al. Iron-mediated retinal degeneration in haemojuvelin-knockout mice. *Biochem J*. 2012;441:599–608.
15. Tawfik A, Gnanaprakasam JP, Smith SB, Ganapathy V. Deletion of hemojuvelin, an iron-regulatory protein, in mice results in abnormal angiogenesis and vasculogenesis in retina along with reactive gliosis. *Invest Ophthalmol Vis Sci*. 2014;55:3616–3625.
16. Martin PM, Gnanaprakasam JP, Roon P, Smith RG, Smith SB, Ganapathy V. Expression and polarized localization of the hemochromatosis gene product HFE in retinal pigment epithelium. *Invest Ophthalmol Vis Sci*. 2006;47:4238–4244.
17. Lin L, Goldberg YP, Ganz T. Competitive regulation of hepcidin mRNA by soluble and cell-associated hemojuvelin. *Blood*. 2005;106:2884–2889.
18. Core AB, Canali S, Babitt JL. Hemojuvelin and bone morphogenetic protein (BMP) signaling in iron homeostasis. *Front Pharmacol*. 2014;5:104.
19. Andriopoulos B Jr, Corradini E, Xia Y, et al. BMP6 is a key endogenous regulator of hepcidin expression and iron metabolism. *Nat Genet*. 2009;41:482–487.
20. He W, Miao FJ, Lin DC, et al. Citric acid cycle intermediates as ligands for orphan G-protein-coupled receptors. *Nature*. 2004; 429:188–193.
21. Sapieha P, Sirinyan M, Hamel D, et al. The succinate receptor GPR91 in neurons has a major role in retinal angiogenesis. *Nat Med*. 2008;14:1067–1076.
22. Favret S, Binet F, Lapalme E, et al. Deficiency in the metabolite receptor SUCNR1 (GPR91) leads to outer retinal lesions. *Aging* (Albany NY). 2013;5:427–444.
23. Nishimura R, Hata K, Ikeda F, et al. The role of Smads in BMP signaling. *Front Biosci*. 2003;8:s275–s284.
24. Liu C, Wu J, Zhu J, et al. Lactate inhibits lipolysis in fat cells through activation of an orphan G-protein-coupled receptor, GPR81. *J Biol Chem*. 2009;284:2811–2822.
25. Taggart AK, Kero J, Gan X, et al. (D)-β-Hydroxybutyrate inhibits adipocyte lipolysis via the nicotinic acid receptor PUMA-G. *J Biol Chem*. 2005;280:26649–26652.
26. Martin PM, Ananth S, Cresci G, Roon P, Smith SB, Ganapathy V. Expression and localization of GPR109A (PUMA-G/HM74A) mRNA and protein in mammalian retinal pigment epithelium. *Mol Vis*. 2009;15:362–372.
27. Joyal JS, Omri S, Sitaras N, Rivera JC, Sapieha P, Chemtob S. Neovascularization in retinopathy of prematurity: opposing actions of neuronal factors GPR91 and semaphorins 3A. *Acta Paediatr*. 2012;101:819–826.
28. Gnanaprakasam JP, Baldowski RB, Ananth S, Martin PM, Smith SB, Ganapathy V. Retinal expression of the serine protease matriptase-2 (Tmprss6) and its role in retinal iron homeostasis. *Mol Vis*. 2014;20:561–574.
29. Ehrlich M, Horbelt D, Marom B, Knaus P, Henis YI. Homomeric and heteromeric complexes among TGF-β and BMP receptors and their roles in signaling. *Cell Signal*. 2011;23:1424–1432.
30. Bandyopadhyay A, Yadav PS, Prashar P. BMP signaling in development and diseases: a pharmacological perspective. *Biochem Pharmacol*. 2013;85:857–864.
31. Wong RW, Richa DC, Hahn P, Green WR, Dunaief JL. Iron toxicity as a potential factor in AMD. *Retina*. 2007;27:997–1003.
32. Ciudin A, Hernandez C, Simo R. Iron overload in diabetic retinopathy: a cause or a consequence of impaired mechanisms? *Exp Diabetes Res*. 2010;2010: pii: 714108.
33. Gnanaprakasam JP, Martin PM, Smith SB, Ganapathy V. Expression and function of iron-regulatory proteins in retina. *IUBMB Life*. 2010;62:3630370.
34. Parrow NL, Fleming RE. Bone morphogenetic proteins as regulators of iron metabolism. *Annu Rev Nutr*. 2014;34:77–94.
35. Hadziahmetovic M, Song Y, Wolkow N, et al. Bmp6 regulates retinal iron homeostasis and has altered expression in age-related macular degeneration. *Am J Pathol*. 2011;179:335–348.

Investigative Ophthalmology & Visual Science